Anomalous moment and anisotropy behavior in Fe_3O_4 films

D. T. Margulies, F. T. Parker, and F. E. Spada
Center for Magnetic Recording Research, University of California at San Diego, La Jolla, California 92093-0401

R. S. Goldman*
Department of Electrical and Computer Engineering, University of California at San Diego, La Jolla, California 92093-0407

J. Li and R. Sinclair
Department of Materials Science, Stanford University, Stanford, California 94305

A. E. Berkowitz
Department of Physics and Center for Magnetic Recording Research, University of California at San Diego, La Jolla, California 92093-0401

(Received 27 July 1995)

Fe_3O_4 films were grown on Si, ⟨100⟩ and ⟨110⟩ MgO, ⟨111⟩ $MgAl_2O_4$, and ⟨0001⟩Al_2O_3 by reactive sputter deposition. X-ray diffraction and TEM studies of the films grown on MgO show they are uniformly strained epitaxial single crystal specimens. Conversion electron Mössbauer spectroscopy (CEMS) spectra for films on all substrates show the presence only of the stoichiometric Fe_3O_4 phase, and values for the hyperfine fields and isomer shifts of the *A* and *B* sites consistent with bulk Fe_3O_4. However, the CEMS spectra exhibit an anomalous out-of-plane moment distribution, although the moments are expected to be in the plane of the film due to the large shape anisotropy. Furthermore, the magnetization remains unsaturated in fields as large as 70 kOe, and torque measurements of films grown on MgO remain unsaturated at 21 kOe. The extrapolated values for the anisotropy, derived from torque curves taken both in and out of the film plane, are much smaller than that required to cause the lack of saturation in high fields and the anomalous CEMS spectra, and are fairly well explained as a combination of crystalline, magnetoelastic, and shape anisotropy of bulk single crystal Fe_3O_4 subjected to in-plane tensile stress. The magnetoelastic anisotropy derived for ideal epitaxial Fe_3O_4 films grown on ⟨100⟩ and ⟨110⟩ MgO, using bulk values for the magnetostriction and elastic constants, agrees well with values determined experimentally. A comparison of films with thicknesses ranging from 0.01 to 6 μm indicates the anomalous behavior to be a volume, as opposed to a surface, effect. The anomalous behavior is exhibited in films grown on other substrates and by other techniques (evaporation and molecular beam epitaxy), and is independent of thickness and deposition conditions. It appears to be an intrinsic property of all Fe_3O_4 films. Possible origins of this behavior are discussed.

INTRODUCTION

The scientific and technological interest in the spinel iron oxide system has led many investigators to examine the magnetic properties and growth of Fe_3O_4 on a variety of substrates using several deposition methods.[1–11] Growth on silicon substrates results in polycrystalline films.[8,10] Growth on ⟨0001⟩ Al_2O_3,[6] ⟨100⟩ MgO,[1–6,9,11] and ⟨110⟩ MgO, (Refs. 4 and 5) results in highly oriented or epitaxial films. Fe_3O_4 grows with ⟨111⟩ orientation on ⟨0001⟩ Al_2O_3, and with the same orientation as the substrate when grown on MgO. Fe_3O_4 and MgO both crystallize with their oxygen atoms in a face-centered-cubic (fcc) crystal lattice, with the distances between rows of oxygen atoms along the ⟨100⟩ directions being 2.106 Å for MgO and 2.099 Å for Fe_3O_4. The close structural match between MgO and Fe_3O_4 suggests that MgO is a good substrate choice for the growth of epitaxial single crystal Fe_3O_4.

The observed magnetic properties of Fe_3O_4 films are, however, puzzling. The magnetization measured in the film plane for Fe_3O_4 films grown on silicon[8] by reactive rf sputtering was unsaturated above 15 kOe, whereas the magnetization is expected to saturate near the anisotropy field H_K of bulk Fe_3O_4, ~310 Oe.[12] Moreover, the presence of a similar anomalous behavior was also observed in oriented Fe_3O_4 films grown on MgO by dc reactive sputtering,[4] as well as in oriented films grown on Al_2O_3 and MgO by evaporation.[6] This paper discusses the structural and magnetic properties of Fe_3O_4 films with a focus on characterizing the anomalous behavior. The unsaturated magnetization at high fields does not appear to be a surface, but rather a volume effect. This behavior is present in both the polycrystalline films grown on Si and the single crystal films grown on MgO. Torque curves measured both in and out of the plane of films grown on MgO are unsaturated at 21 kOe. However, the extrapolated values of the anisotropy constants are much less than the magnitude which would be needed to cause the lack of saturation of the magnetization. Furthermore, the extrapolated anisotropy is fairly well explained as a combination of crystalline, magnetoelastic, and shape anisotropy of bulk single crystal Fe_3O_4 subjected to in-plane tensile stress. The anomalous behavior seems to be an intrinsic property of Fe_3O_4 films which is apparently independent of deposition technique.

TABLE I. Deposition conditions of the samples listed and relevant characterization parameters. Films with the same number and letter label were grown during the same deposition, while films with only the same number label were grown consecutively. Listed parameters include the O_2 pressure during deposition $P(O_2)$, the deposition rate R, the substrate to target distance d, the film thickness t, the magnetization at 70 kOe M, the Verwey transition temperature T_v (which is measured along the ⟨100⟩ direction for both the ⟨100⟩ and ⟨110⟩ oriented samples), the anisotropy constants K_1 and K_u measured at 21 kOe, the Mössbauer polarization p, and the effective angle θ_{eff} calculated from p. For the measurements of T_v, the majority of the change in the magnetization generally takes place over a 1 K temperature range. If the decrease in the magnetization takes place over a 2–4 K region then T_v is designated by "*" and if the decrease in the magnetization takes place over a ~10 K region then T_v is designated by "**." The uncertainties in the last digit for p and θ_{eff} are given in parenthesis next to the values. The measured p and θ_{eff} parameters for the MBE grown film are also listed. The value for θ_{eff} for the film grown by evaporation is taken from Ref. 6.

	$P(O_2)$ (mtorr)	Substrate	R (Å/min)	d (cm)	t (Å)	M (emu/cc)	T_v (K)	K_1 (10^4 ergs/cc)	K_u (10^5 ergs/cc)	p	θ_{eff} (deg)
1*a*	0.09	⟨100⟩MgO	123	13	4280	465	115.5	−7.76		0.71(2)	46.4(5)
1*b*	0.09	⟨100⟩MgO	123	13	1610	468	110.5	−6.30		0.79(1)	48.8(3)
1*c*	0.09	⟨100⟩MgO	123	13	540	431	108.0*	−4.20		1.00(2)	54.8(6)
1*d*	0.09	⟨100⟩MgO	123	13	134	422	92**	−2.42			
1*a*	0.09	⟨110⟩MgO	123	13	4280	450	116.5		−3.84	1.57(3)	69.7(9)
1*b*	0.09	⟨110⟩MgO	123	13	1610	477			−4.91	1.58(2)	70.0(4)
1*c*	0.09	⟨110⟩MgO	123	13	540	438	111.0*		−5.19	1.60(2)	70.7(7)
1*d*	0.09	⟨110⟩MgO	123	13	134	392	98**		−3.80		
2*a*	0.12	⟨100⟩MgO	80	13	3000	472	111.7	−6.93		0.96(2)	53.7(5)
2*b*	0.12	⟨100⟩MgO	80	13	1500		112.0	−7.46			
2*c*	0.12	⟨100⟩MgO	80	13	500	449	102.0*	−6.06		1.06(2)	56.4(6)
3*a*	0.12	⟨100⟩MgO	103	13	4520	470	113.5	−8.85		0.74(2)	47.3(5)
3*b*	0.12	⟨100⟩MgO	103	13	132	414		−4.08			
3*b*	0.12	⟨110⟩MgO	103	13	132	451			−3.20		
4*a*	0.12	⟨100⟩MgO	~138	13	6.63 μm	437	107.5	−3.77		0.94(1)	53.1(4)
4*a*	0.12	⟨110⟩MgO	~138	13	6.63 μm	453	110.0*		−2.65	1.54(3)	68.9(7)
5*a*	0.12	⟨100⟩MgO	67	18	3090	468	105.5	−7.84			
5*a*	0.12	⟨111⟩$MgAl_2O_4$	67	18	3090					1.41(4)	55.6(4)
5*a*	0.12	⟨0001⟩Al_2O_3	67	18	3090					1.07(1)	56.6(4)
6*a*	0.12	⟨100⟩MgO	62	18	2500	454	102.0	−6.45		0.88(1)	51.4(4)
6*a*	0.12	Si	62	18	2500	462	104.0*			1.03(1)	55.6(4)
					Other growth techniques						
MBE		⟨100⟩MgO			10000		120.5			0.76(4)	48(1)
Evaporation (Ref. 6)		⟨100⟩MgO			1000						47.6

EXPERIMENTAL PROCEDURES

Fe_3O_4 films were deposited onto polished ⟨111⟩ $MgAl_2O_4$ spinel, ⟨100⟩ and ⟨110⟩ MgO, Si, and ⟨0001⟩ α-Al_2O_3 substrates using dc magnetron reactive sputtering from an Fe target with 99.95% purity in an Ar-O_2 gas mixture. The substrates were fixed to a copper plate which was attached to a heater. A thermocouple attached to the copper plate on the same side as the substrates determined the substrate temperature. The substrates were preheated for 1 h at 500 °C, in a background pressure near 3×10^{-7} torr, before deposition at 500 °C. Following deposition, first the O_2 and then the Ar gas flow was shut off and the samples were cooled to near room temperature in vacuum. During deposition the Ar pressure was adjusted to 2.00 mtorr and the current was controlled at 0.250 A. The O_2 pressures, deposition rates, and the target-to-substrate distances for the films discussed in this study are listed in Table I. Samples will be identified by the labels listed in this table. Other samples evaluated included a bulk single crystal Fe_3O_4 specimen grown from the melt by Dr. F. Bruni at Oak Ridge National Labs, and a 1 μm film grown via molecular-beam epitaxy (MBE) by Lind *et al.*.[1–3]

Thicknesses of films under 600 Å were measured by low angle x-ray diffraction.[13] This established the deposition rate which was used to determine the thickness of the other films in the series with an uncertainty estimated to be ~1%. A Dektak profilometer, calibrated with ~0.4 μm films, was used to determine the thickness of the ~6 μm films. Uncertainties in the film areas were estimated to be less than 1%.

Magnetization data were taken with a superconducting quantum interference device (SQUID) magnetometer, which was calibrated using Pd and Ni standards. Corrections were made for the deviation of the sample size from a point source. Including this correction, and sample remounting, the estimated uncertainties in the magnetic moments are ~1%. The susceptibilities of blank ⟨100⟩ MgO, ⟨110⟩ MgO, and Si substrates, with ~0.2 mm thicknesses, were measured and their magnetic signals were subtracted from the magnetization data. The standard deviation obtained from the measured susceptibilities of three blank ⟨100⟩ MgO substrates was 1.1%. This is considered to be the uncertainty in the back-

ground subtraction. The diamagnetic contribution to the measured moment from the MgO at 70 kOe is almost four times the ferrimagnetic contribution of a ~130 Å film. Therefore, the uncertainty in the absolute magnetization of the films, one standard deviation, increased from 2% to 5% as the film thickness decreased from ~4000 to ~130 Å. Field cooling experiments were performed by first magnetizing the sample at 70 kOe lowering to 10 kOe while still at 300 K, cooling to 10 K and increasing to the measurement temperature in the 10 kOe field, and then increasing the field to 70 kOe before measuring magnetization versus field.

Torque magnetometer scans were taken at room temperature from $\theta=-90°$ to 460° and back to $-90°$ within a 20 min time period, where θ is the angle of the applied field referenced to an arbitrary direction in the crystal. The torque was calibrated using the shape anisotropy of a fine Ni wire. The standard deviation in the torque calibration using three wires of different lengths was 0.6%. The average of the clockwise and counter-clockwise curves was used to determine Fourier transforms of the torque data. The $\sin 2\theta$ and $\sin 4\theta$ terms used to calculate the anisotropy constants were found to be reproducible to within 1%, including sample remounting.

The conversion electron Mössbauer spectroscopy (CEMS) measurements were performed using a flowing He-methane gas detector at 296 K and zero applied field. The source was ^{57}Co in Rh. The reported isomer shifts are relative to Fe metal, and the velocity was calibrated using Fe metal.

Structural characterization included (1) symmetric Bragg reflection x-ray-diffraction (XRD) measurements (θ-2θ scans) performed with a Rigaku diffractometer; (2) x-ray rocking curve measurements (θ scans) measured with a high resolution x-ray diffractometer using Cu $K_{\alpha 1}$ radiation monochromated by four Ge⟨220⟩ crystals; (3) high resolution TEM studies of cross-section specimens prepared using the Bravman-Sinclair method[14] with ion milling at 77 K.

RESULTS

Structural characterization

We have completed an x-ray-diffraction study of the ⟨100⟩ oriented film 1*a* and the ⟨110⟩ oriented film 1*b* using a four-crystal diffractometer. The details of this study will be reported elsewhere and only a summary of the results are presented here. By studying the 800 reflection under different geometries, as well as reflections of the form ⟨840⟩ and ⟨622⟩, specimen 1*a* was shown to be a single crystal with a tetragonally-distorted unit cell [bulk Fe_3O_4 has the cubic spinel structure with lattice parameter $a_0=8.3967$ Å (Ref. 15)]. Taking an average from these various reflections, the lattice parameter along the direction normal to the film plane is 8.3726(2) Å and the lattice parameters of the orthogonal in-plane directions are both 8.4259(3) Å, where the uncertainty in the last digit is enclosed in parentheses. The in-plane lattice parameters are, within uncertainty, twice that of the MgO substrate[15] (4.213 Å). This established the coherent or pseudomorphic growth of Fe_3O_4 on the MgO substrate, which produces strain in the film. Broadening of the film peaks was found to be small. For example, Fig. 1 shows a representative rocking curve of the planes parallel to the film surface. The full width at half maximum (FWHM) of the Fe_3O_4 800 reflection is 0.0112(5)°, while the FWHM of the 400 MgO reflection is 0.0055(1)°. Similar diffraction profiles were found for the asymmetric reflections. The small breadth of the film reflections indicates that the *d* spacing is relatively uniform throughout the 4280 Å film, with little relaxation toward the bulk *d* spacing. The ⟨110⟩ oriented film was also found to be an epitaxial single crystal growing coherent with the MgO, resulting in a tetragonal distortion, with little peak broadening.

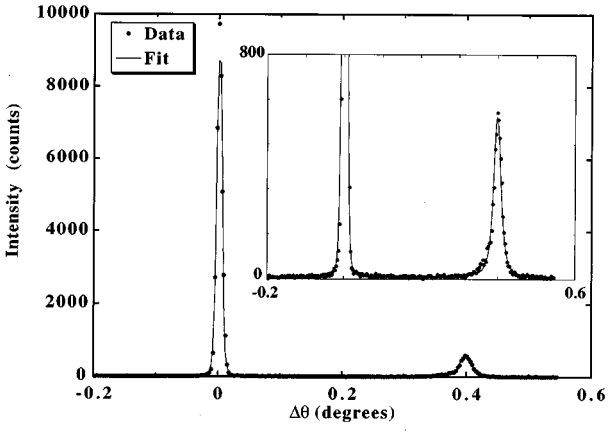

FIG. 1. Rocking curve of the symmetric 800 Fe_3O_4 and 400 MgO reflections for the film 1*a* grown on ⟨100⟩ MgO. $\Delta\theta$ is the difference between the measurement angle and the angle at which the substrate reflection is at maximum intensity. The inset shows the lower intensity region of the rocking curve to facilitate comparison between the FWHM of the Fe_3O_4 and MgO reflections. The data are the points and the line is the fit.

A cross section of the ⟨100⟩ oriented film 2*b* was studied with high resolution transmission electron microscopy. A representative micrograph is shown in Fig. 2. Other micrographs obtained over a greater than 2 μm region were similar. The diffraction pattern is consistent with an epitaxial single crystal spinel Fe_3O_4 film. Analysis of the lattice fringes also indicates a single crystal epitaxial film. The Fe_3O_4/MgO interface appears relatively sharp.

d spacings normal to the film plane were measured using θ-2θ scans. A discussion of these measurements on films grown on MgO has already been presented elsewhere.[4,5] The lattice parameters for the films grown on Si, ⟨0001⟩ α-Al_2O_3, and ⟨111⟩ $MgAl_2O_4$, are 8.381, 8.386, and 8.372 Å, respectively, as derived from the 311, the 444, and the 444 spinel *d* spacings normal to the film plane. The lattice parameters for the ⟨100⟩ and ⟨110⟩ oriented 6.6 μm films are 8.376 and 8.380 Å, respectively, as calculated from the 800 and 440 spinel *d* spacings normal to the film plane. It is noteworthy that the *d* spacings of the 6.6 μm films have relaxed only slightly toward the bulk value of 8.3967 Å. The uncertainty in all these measurements is about ± 0.002 Å. The XRD spectra for the film grown on ⟨111⟩ $MgAl_2O_4$ also exhibited the 511 and 751 reflections of both the film and the substrate. Qualitatively, these reflections were as intense and as sharp as the 111 reflections indicating quite large substrate regions having ⟨511⟩ and ⟨751⟩ orientations.

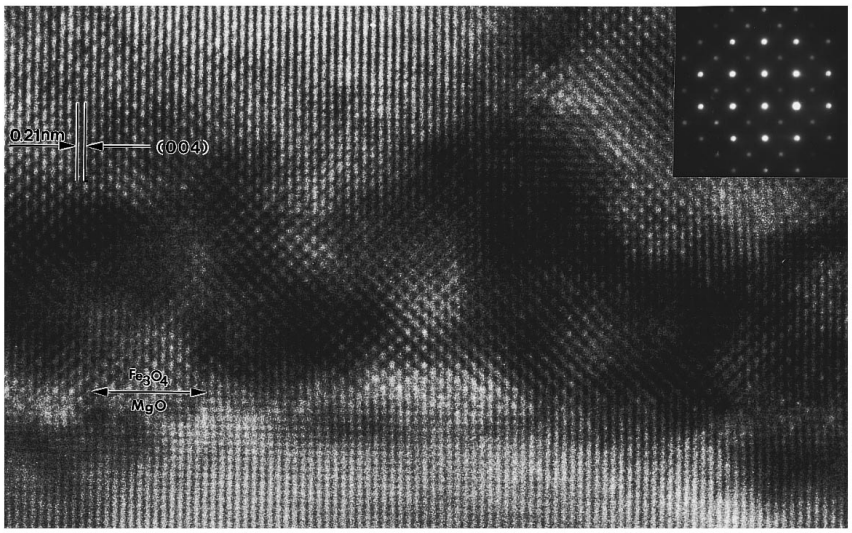

FIG. 2. High resolution TEM lattice image along a ⟨100⟩ zone axis of the Fe_3O_4 film $2b$ grown on ⟨100⟩ MgO. A selected area diffraction pattern of the film is shown in the upper right corner.

Magnetization

High field in-plane magnetization data for various Fe_3O_4 specimens are shown in Fig. 3. The magnetization (M) is shown as the field (H) is increased to 70 kOe and then decreased; no hysteresis at these fields is observed. The most striking feature of the data is the lack of saturation of the films in a 70 kOe field, regardless of substrate; in contrast, the bulk single crystal sample saturates readily. The films are expected to saturate near 310 Oe, the anisotropy field of bulk Fe_3O_4. The bulk specimen is irregularly shaped, introducing some shape anisotropy, which is probably why it does not saturate until $H \sim 2$ kOe.

The approach to saturation at high fields was fit by the equations $M = M_s(1 - a/H)$ and $M = M_s(1 - b/H^2)$ and was found to be better described by the former. It is noteworthy that the former field dependence of M is attributed to defects present in the material and the latter is attributed to crystal anisotropy.[16] The bulk value for M_s is 471 emu/cc.[17] By extrapolation of the data in Fig. 3, we obtain M_s values of 474, 474, 473, and 476 emu/cc for the films grown on Si, ⟨110⟩ MgO (⟨110⟩ in-plane direction), ⟨110⟩ MgO (⟨100⟩ in-plane direction), and ⟨100⟩ MgO (⟨100⟩ in-plane direction), respectively. Although the uncertainty in the absolute magnetization is 2%, the relative magnetization uncertainty between field points for the same sample is smaller than the data point size in the figure, and the statistical uncertainties (not shown) are smaller than the point size. The polycrystalline film grown on Si has the same high field behavior as the single crystal film grown on ⟨100⟩ MgO. The single crystal film grown on ⟨110⟩ MgO exhibits a slower approach to saturation for both the ⟨110⟩ and ⟨100⟩ in-plane directions relative to the films grown on Si and ⟨100⟩ MgO, but the high field behavior is qualitatively the same for these two directions. No directional dependence in the high field susceptibility could be seen in the in-plane $M-H$ curves measured by vibrating sample magnetometry (VSM) in applied fields up to 24 kOe along many different crystallographic directions. The $M-H$ curves measured perpendicular to the film plane were unsaturated at 24 kOe. No time dependence was observed for the high field magnetization. σ_s for the bulk specimen in Fig. 3 is 95 ± 1 emu/g, which is slightly larger than reported by Aragon.[18] In Fig. 3 the saturation magnetization of the bulk sample was normalized to 471 emu/cc to facilitate comparison with the films. The $M-H$ curve for this specimen was taken along an unknown crystal direction. Another important point is that the 1 μm film grown by MBE also exhibits a much slower approach to saturation than the bulk specimen; for example, measurements in our laboratory show the magnetization along an in-plane ⟨100⟩ direction for this film reaches 92% of its extrapolated value (476 emu/cc) at 10 kOe and 98% of its extrapolated value at 70 kOe.

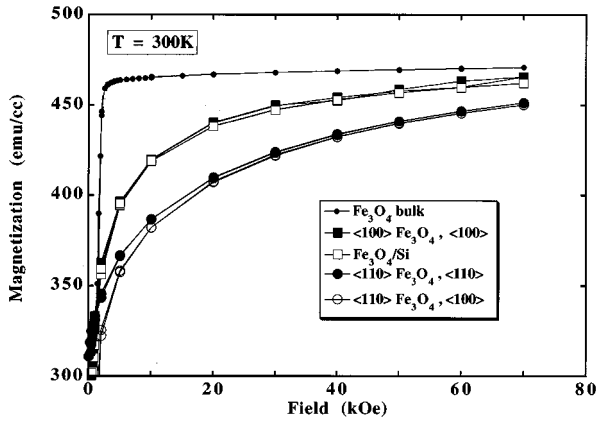

FIG. 3. Magnetization measured in the film plane as a function of field for Fe_3O_4 films grown on Si (film $6a$), ⟨100⟩ MgO ($1a$), and ⟨110⟩ MgO ($1a$). The crystallographic direction along which the field is applied is indicated beside each film in the figure. The bulk specimen is measured along an unknown crystal direction. The magnetization axis is offset to facilitate observation of the high field data. The lines are visual guides.

The approach to saturation as a function of temperature for the 0.3 μm film $5a$ grown on ⟨100⟩ MgO is shown in Fig. 4. For this sample the substrate used to measure the MgO susceptibility as a function of temperature was the same substrate on which the film was deposited. Therefore, the MgO signal could be directly subtracted. The magnetization is shown as the field is increased and then decreased. At high fields these loops are closed within experimental uncertainty. Although the 10 and 100 K data show a slightly slower ap-

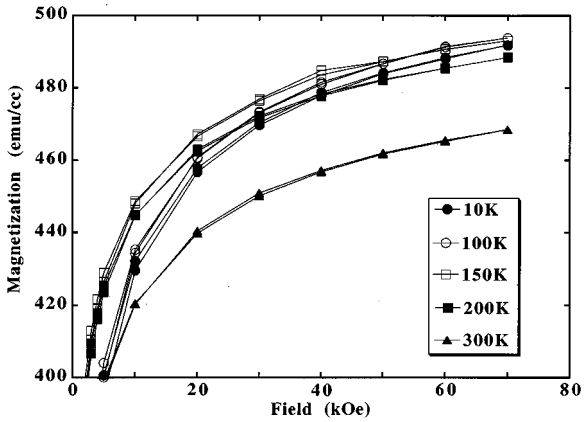

FIG. 4. Magnetization measured in the film plane along a ⟨100⟩ direction as a function of field and temperature for the 0.3 μm Fe_3O_4 (film 5a, Table I) grown on ⟨100⟩ MgO. For this specimen the magnetization as a function of field and temperature for the MgO substrate was measured before deposition on that substrate. This background signal is directly subtracted. The magnetization is shown as the field is increased and then decreased. At high fields these loops are closed within experimental uncertainty. The lines are visual guides.

proach to saturation than the higher temperature data, there is no strong temperature dependence of the saturation behavior. A strong temperature dependence might be expected if difficulty in achieving saturation was due to magnetocrystalline anisotropy.[19] The temperature dependence of M_s for the ⟨100⟩ oriented film 5a is qualitatively very close to that of bulk Fe_3O_4. For example, the values of $M(300\ \mathrm{K})/M(10\ \mathrm{K})$ for the bulk crystal and the film, where M is the magnetization value at 70 kOe, are 0.945(1) and 0.951(3), respectively.

High field in-plane magnetization data at 300 K for films with various thicknesses are shown in Fig. 5. The important point of this figure is that the slow approach to saturation is present in films of all thicknesses, with only a slight thickness dependence observed. A decrease in the magnetization at 70 kOe with decreasing thickness is indicated by the results summarized in Table I and Fig. 5. However, the observed magnetizations at 70 kOe for all films measured are within a range of 2–3 standard deviations, so the reality of this decrease is at the limit of statistical significance. Finally, the coercivity of the ⟨100⟩ oriented films at 300 K was near 85 Oe for the ~4500 Å films and increased with decreasing thickness to near 150 Oe for the ~130 Å films, while the bulk specimen exhibits 0 ± 5 Oe coercivity.

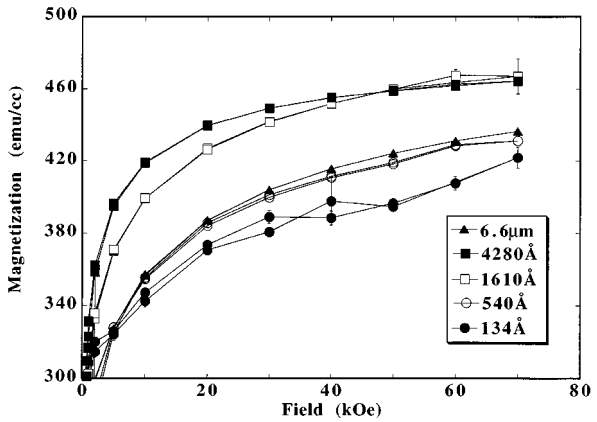

FIG. 5. Magnetization measured in the film plane along a ⟨100⟩ direction as a function of field and thickness for the series of Fe_3O_4 films 1a–1d (Table I) grown on ⟨100⟩ MgO and the 6.6 μm Fe_3O_4 film 4a grown on ⟨100⟩ MgO. The lines are visual guides.

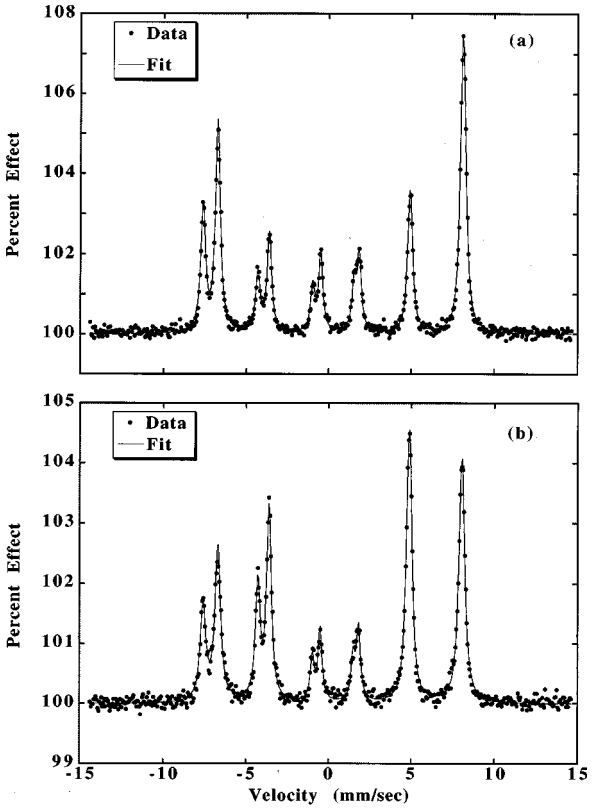

FIG. 6. CEMS spectra for the 0.43 μm Fe_3O_4 film 1b grown on ⟨100⟩ MgO (a) and the 0.16 μm Fe_3O_4 film 1b grown on ⟨100⟩ MgO (b). The data (points) were taken at room temperature and in zero applied field and the line is the fit.

Conversion electron Mössbauer spectroscopy

CEMS spectra and the associated fits for the 4280 Å ⟨100⟩ oriented film 1a and the 1610 Å ⟨110⟩ oriented film 1b are shown in Fig. 6. In Fe_3O_4, iron occupies two crystallographic sites which exhibit six Mössbauer lines each. The tetrahedral A site contains only Fe^{3+} ions and the octahedral B site contains equal numbers of Fe^{2+} and Fe^{3+} ions. The hyperfine fields, the isomer shifts, and the relative occupancy of the A and B sites are derived from fits to the data. The respective values of these parameters for the A and B sites in bulk Fe_3O_4 are 491 and 462 kOe, 0.27 and 0.67 mm/s and 1:2.[20] These values were obtained for all films listed in Table I, within the uncertainty of ±2 kOe for the hyperfine fields, ±0.01 mm/s for the isomer shifts, and 2% for the relative occupancy. The variation in the measured value for the hyperfine fields partially results from variations in the solid angle subtended by the absorber. It is noteworthy that no superparamagnetic component is observed in the CEMS spectra. This result, coupled with the temperature dependence of the approach to saturation and structural character-

ization, eliminates the possibility that the lack of saturation arises from superparamagnetic regions in the films.

The relative intensity of the lines in each sextet is given as $3{:}2p{:}1{:}1{:}2p{:}3$, where the polarization $p=2\sin^2\theta/(1+\cos^2\theta)$, and θ is the equivalent single orientation angle between the magnetic hyperfine field and the γ-ray direction; $p=1$ for three-dimensional random moment orientation, $p=2$ for in-plane moment alignment, and $p=0$ for a perpendicular moment alignment. A Fe_3O_4 thin film has a shape anisotropy constant $K_s=2\pi M_s^2=1.39\times10^6$ ergs/cc ($H_K=2K_s/M_s=5.9$ kOe) (Ref. 12) which is an order of magnitude larger than the crystalline anisotropy. The moments should therefore lie in the plane of the film. However, this is not observed in our Fe_3O_4 films of all thicknesses and grown on different substrates, as is seen from Fig. 6 and from Table I, where the values for p, as well as the effective angles calculated from p, are shown for all films studied. Similar behavior is also observed in Fe_3O_4 films grown by other deposition techniques (e.g., MBE and evaporation), as shown in Table I. The value for p was observed to be independent of the magnetic history of the specimen. CEMS spectra were measured at zero applied field on the $\langle100\rangle$ oriented film $1d$ after (1) applying a 24 kOe field in the film plane, (2) applying a 24 kOe field perpendicular to the film plane, (3) dc demagnetization, (4) ac demagnetization; all values for p were found to be the same.

Anisotropy

Figure 7(a) compares torque curves measured at 21 kOe and room temperature within the film planes of the 4520 and 132 Å $\langle100\rangle$ oriented specimens ($3a$,$3b$). For the (100) plane of a cubic crystal the torque $L=-(K_1/2)\sin4\theta$.[21] This symmetry is found in our $\langle100\rangle$ oriented specimens [Fig. 7(a)], with $\langle110\rangle$ being the easy directions[4] within the film plane which is of the form {100}, as expected for bulk Fe_3O_4. The measured K_1 values for the $\langle100\rangle$ films $1a-1d$ are plotted in Fig. 8(a) versus applied magnetic field. As with the magnetization data, the measured values for K_1 remain unsaturated in abnormally high fields. The highest unsaturated measured values for K_1 (Table I) are approaching those of bulk Fe_3O_4 [$K_1=-1.10\pm0.08\times10^5$ ergs/cc (Ref. 17)]. For example, approximating the approach to saturation as being proportional to $1/H$, a value of -1.0×10^5 ergs/cc is obtained for film $1a$. However, there is a much stronger dependence on the film thickness for both the magnitude and the field dependence of K_1 than for the magnetization; for the thinner films K_1 is more difficult to saturate in high fields and the magnitude is smaller.

Figure 7(b) compares torque curves measured at 21 kOe and room temperature within the film planes of the 4280 and 132 Å $\langle110\rangle$ oriented specimens ($1a$,$3b$). For the $\langle110\rangle$ oriented films, in-plane torque curves show that the expected crystalline anisotropy is dominated by an anisotropy which has a $\sin2\theta$ functional form for the torque. In this case, the film plane is of the form {110} (in which the $\langle110\rangle$ and $\langle100\rangle$ directions are orthogonal) and the $\langle110\rangle$ direction is the easy direction, while the $\langle100\rangle$ is hard. Since the $\sin2\theta$ functional form for the torque is similar to a uniaxial anisotropy, we label the anisotropy constant calculated from these torque curves as K_u. The largest value measured for K_u is -5.19×10^5 ergs/cc, corresponding to $H_K=2.2$ kOe, and the

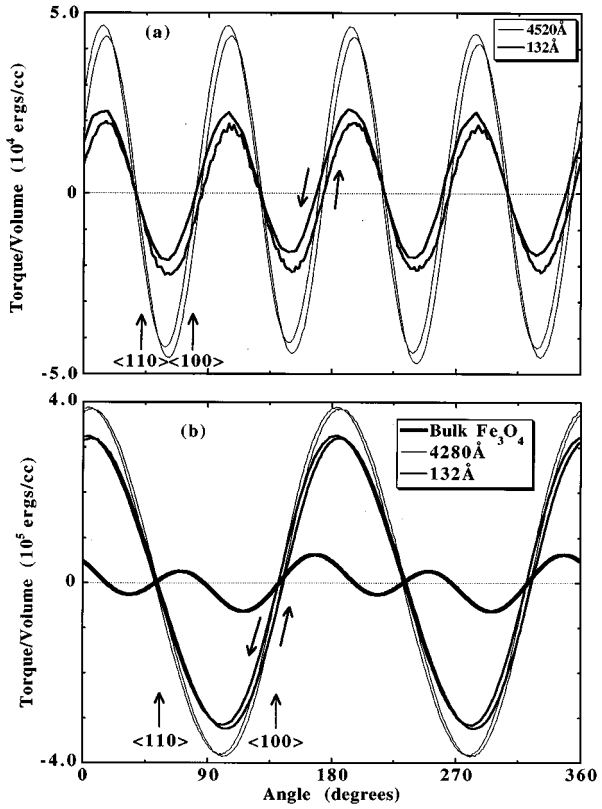

FIG. 7. Torque curves for Fe_3O_4 films $3a$, $3b$ (Table I) grown on (a) $\langle100\rangle$ MgO and films $1a$,$1d$ (Table I) grown on (b) $\langle110\rangle$ MgO, respectively. The data were taken at room temperature and in a magnetic field of 21 kOe. Both the clockwise and counterclockwise curves are shown and crystallographic directions are indicated in the figure. In (b), the curve for the bulk specimen was calculated (Ref. 21) using the bulk values (Ref. 17) for K_1.

negative value will be explained in the following section. K_u is plotted as a function of thickness and field for the $\langle110\rangle$ oriented films in Fig. 8(b). As with K_1 for the $\langle100\rangle$ oriented films, the measured values of K_u become more difficult to saturate as the thickness decreases. Even though a $\sin4\theta$ crystalline term is not noticeably apparent in the torque curves [Fig. 7(b)], the Fourier transform of the curve for film $1a$ gives a $\sin4\theta$ term which would correspond to[21] $K_1=-4.69(1)\times10^4$ ergs/cc. However, the magnitude of this $\sin4\theta$ term is also strongly affected by the asymmetry of the $\sin2\theta$ term arising from lack of saturation. The significance of the $\sin4\theta$ term is therefore not clear and it will not be considered further.

Out-of-plane torque curves were also measured such that the plane of measurement included both a direction within the specimen plane and a direction normal to the film surface. The planes considered are illustrated in Fig. 9. For $\langle110\rangle$ oriented specimens [Fig. 9(a)] the film surface is defined as the (110) plane and torque curves were measured within the (110) plane which contains the [110] direction normal to the film surface and the in-plane [001] direction; measurements were also made within the (001) plane which contains the [110] direction normal to the film surface and the in-plane [110] direction. For $\langle100\rangle$ oriented specimens [Fig. 9(b)] the film surface is defined as the (001) plane and torque curves were measured in the (110) plane which con-

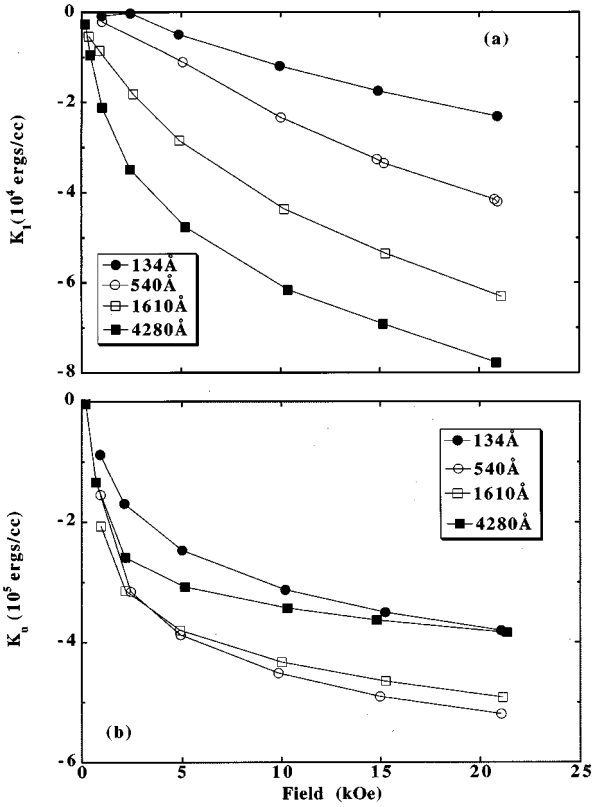

FIG. 8. (a) The measured values of K_1 as a function of field and thickness for the series of Fe_3O_4 films $1a-1d$ (Table I) grown on ⟨100⟩ MgO. (b) The measured values of K_u as a function of field and thickness for the series of Fe_3O_4 films $1a-1d$ (Table I) grown on ⟨110⟩ MgO. The values for K_1 and K_u are derived from the amplitude of the $\sin 4\theta$ and $\sin 2\theta$ components, respectively, of the Fourier transform of the average of the clockwise and counter-clockwise curves. The lines are visual guides.

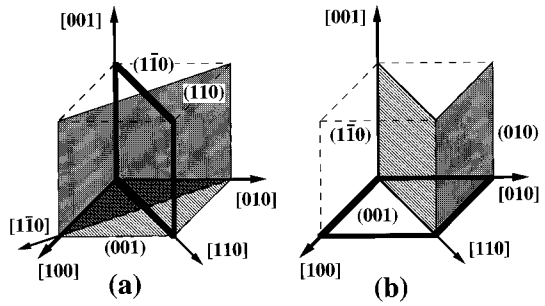

FIG. 9. Schematic representation of crystallographic orientation of torque measurement planes. The specimen film planes are outlined with bold perimeters. The planes in which out-of-plane torque measurements were made are shaded or ruled. (a) ⟨110⟩ oriented specimen; the direction normal to the film surface is defined as [110]. (b) ⟨100⟩ oriented specimen; the direction normal to the film surface is defined as [001].

tains the [001] direction normal to the film surface and the in-plane [110] direction; measurements were also made within the (010) plane which contains the [001] direction normal to the film surface and the in-plane [100] direction. All resulting torque curves exhibited $\sin 2\theta$ functional dependence with the easy axis lying in the film plane, and were unsaturated with a field dependence similar to K_u of the ⟨110⟩ oriented films [Fig. 8(b)]. Table II lists a summary of the measured unsaturated and extrapolated values for the anisotropy constants, as well as calculated values described in the next section.

The separations between the clockwise curves and the counter-clockwise curves indicate the presence of rotational hysteresis, W_r, in fields as high as 21 kOe. We further observe that W_r is a function of the rate of rotation of the magnet (ω) and was measured to decrease by ~20% when ω is changed from 2×10^{-2} rad/sec to 8×10^{-3} rad/sec. Also, when the rotation is stopped the torque is observed to be time dependent and the direction of the decay is dependent upon the direction of rotation before the stopping point; the decay direction is such as to decrease the separation between the

TABLE II. A summary of measured, extrapolated, and calculated values of anisotropy constant K at 296 K from torque curves taken on the ⟨110⟩ and ⟨100⟩ oriented Fe_3O_4 specimens grown on MgO (films $1a$, Table I). The extrapolated values (K_{ext}) are determined by fitting the approach to saturation of the measured values (K_{meas}) with equation $K_{meas}=K_{ext}(1-a/H)$. The tabulated measured values are determined from curves taken at 21 kOe. Also listed are the resulting anisotropy fields H_K. The calculated anisotropy is an addition of magnetocrystalline, magnetoelastic, and shape anisotropies of a Fe_3O_4 single crystal subjected to an in-plane tensile stress (see text). All terms represent anisotropy constants with $\sin 2\theta$ dependence for the torque ($H_K=|2K_u/M_s|$) except those marked by "*" which represent the cubic magnetocrystalline anisotropy constant $K_1(H_K=-4K_1/3M_s)$.[12] The film plane is defined as the (110) plane for ⟨110⟩ oriented film and the (001) plane for the ⟨100⟩ oriented film. The torque curves measured in the film plane are designated by "*i*" and the curves measured in planes orthogonal to the film surface are designated by "*o*." For the out-of-plane torque curves the easy axis is always in the film plane, and for the in-plane torque curves the easy axes are the ⟨110⟩ directions (see text).

		Measured anisotropy		Extrapolated anisotropy		Calculated anisotropy	
Film orientation	Plane	K (10^5 ergs/cc)	H_K (kOe)	K (10^5 ergs/cc)	H_K (kOe)	K (10^5 ergs/cc)	H_K (kOe)
⟨110⟩	$(\bar{1}\bar{1}0)i$	−3.84	1.6	−4.3	1.8	−8.11	3.4
	$(001)o$	17.4	7.4	21.2	9.0	27.3	11.6
	$(110)o$	13.7	5.8	16.9	7.2	19.2	8.2
⟨100⟩	$(00\bar{1})i$	−0.776*	0.22*	−1.01*	0.29*	−1.1*	0.31*
	$(\bar{1}10)o$	11.7	4.96	13.0	5.52	11.2	4.75
	$(010)o$	11.5	4.89	12.8	5.44	10.9	4.63

clockwise and the counter-clockwise curves. No such behavior was observed with the Ni calibration standard, showing this phenomenon not to be an experimental artifact.

The presence of rotational hysteresis usually indicates the presence of irreversible changes in the magnetization occurring at the magnetic field of observation,[22] but the $M-H$ curves of the films at 20 kOe are closed (Fig. 1), even though they are unsaturated, indicating no irreversible changes occurring in the magnetization at that field. It has been shown[23–25] that bulk $Fe_{3(1-\delta)}O_4$ specimens with small deviations from stoichiometry $\delta \sim 3\times10^{-4}$, as will be indicated in a later section may also be the case in the films, exhibit magnetic after-effect phenomena at 300 K. The relaxation which occurs is identified with jumps of Fe ions into vacant sites of the Fe lattice, leading to a reorientation of the symmetry axis of the trigonally-distorted vacancies.[25] Van Groenou *et al.*[26] derived the expected changes in torque curves if magnetic aftereffect is occurring during torque measurements and his model predicts the presence of a time dependent W_r at abnormally high fields similar to what is observed in these films. This behavior may not be unique to thin films of Fe_3O_4 which indicates that it may not be related to the anomalous behavior.

Magnetoelastic anisotropy

The relatively large amount of strain present in the films and the added anisotropy with $\sin 2\theta$ dependence for the torque measured in the ⟨110⟩ oriented films suggests the importance of magnetoelastic energy in the films. The anisotropy arising from magnetoelastic energy or the strain can be derived from the equation for the magnetoelastic energy, $E_{\rm me}$, which for a cubic crystal is given by the relation[27]

$$E_{\rm me}=-(3/2)\lambda_{100}\sigma(\alpha_1^2\gamma_1^2+\alpha_2^2\gamma_2^2+\alpha_3^2\gamma_3^2) -3\lambda_{111}\sigma(\alpha_1\alpha_2\gamma_1\gamma_2+\alpha_2\alpha_3\gamma_2\gamma_3+\alpha_3\alpha_1\gamma_3\gamma_1). \quad (1)$$

Here, σ is the stress, α_i are direction cosines of M_s, γ_i are the direction cosines of σ, and λ_{hkl} are the magnetostriction coefficients. The ⟨100⟩ and ⟨110⟩ oriented films are measured to be under a tetragonal distortion with a compressive strain normal to the film surface and tensile strain in the film plane. Therefore, we will model the stress tensor of our system as being composed of two orthogonal stresses in the plane of the film with magnitudes such that the resulting strain is that arising from perfect epitaxy of Fe_3O_4 on MgO.

The added anisotropy resulting from this stress model is determined by the relation $L_{\rm me}=-dE_{\rm me}/d\theta$ where $L_{\rm me}$ is the torque arising from magnetoelastic energy, and θ is the angle between M_s and a reference direction in the film plane. We first consider the ⟨110⟩ oriented specimens and define the (110) spinel plane as the film plane for our description of how the torque varies as M_s rotates in that plane. This particular choice places the orthogonal [110] and [001] directions in the film plane; σ_1' and σ_3' are the respective principle stresses along these directions. We use the tensor relation $\varepsilon_i=s_{ij}\sigma_j$, where σ_j is the stress tensor, ε_i is the strain tensor, and s_{ij} are the known[17] compliances of bulk Fe_3O_4.

The calculation of the magnetoelastic anisotropy in the $(1\bar{1}0)$ spinel plane using the stress model described above involves a transformation of coordinate systems.[28] When this is accomplished the equations for the strains are

$$\varepsilon_1'=(s_{11}+s_{12}+s_{44}/2)\sigma_1'/2+s_{12}\sigma_3', \quad (2)$$

$$\varepsilon_2'=(s_{11}+s_{12}-s_{44}/2)\sigma_1'/2+s_{12}\sigma_3', \quad (3)$$

$$\varepsilon_3'=s_{12}\sigma_1'+s_{11}\sigma_3', \quad (4)$$

where ε_i' are the strains along the [110], $[1\bar{1}0]$, [001] directions, respectively. The strains in the [110] and [001] directions, ε_1' and ε_3', respectively, are now set equal to the strain which would result along the in-plane directions if Fe_3O_4 were growing epitaxially on MgO ($\varepsilon=+0.00349$). This permits calculation of σ_1' and σ_3'. Using this result, and bulk values for the magnetostriction constants,[17] the anisotropy resulting from the strain for the desired measurement plane is obtained.[4]

The added anisotropies in the $(1\bar{1}0)$, (001), and (110) planes arising from magnetoelastic coupling are calculated to have $\sin 2\theta$ dependences for the torque in each of the planes with the following magnitudes:

$$(3/4)\sigma_1'(\lambda_{100}-\lambda_{111})-(3/2)\lambda_{100}(\sigma_1'-\sigma_3') = -8.11\times10^5 \ \text{ergs/cc}, \quad (5)$$

$$|(3/2)\lambda_{111}\sigma_1'| = 1.33\times10^6 \ \text{ergs/cc}, \quad (6)$$

$$|(3/4)\sigma_1'(\lambda_{100}+\lambda_{111})-(3/2)\lambda_{100}(\sigma_1'-\sigma_3')| = 5.23\times10^5 \ \text{ergs/cc}. \quad (7)$$

The corresponding H_K values are 3.4, 5.7, and 2.2 kOe. The easy axes for the torque curves in the above planes are along the in-plane directions [110] for the (110) plane, [110] for the (001) plane, and [001] for the (110) plane. For the (110) plane, the negative value of K_u, which is determined from the magnetoelastic energy equation, signifies that [110] is the easy direction; if K_u were greater than zero then the orthogonal [001] direction would be easy.[4] The shape anisotropy term $2\pi M_s^2=1.39\times10^6$ ergs/cc must be included in out-of-plane torque curves. Therefore, with the addition of $2\pi M_s^2$ to Eqs. (6) and (7), the calculated magnitudes for the anisotropy constants in the (001) and (110) planes are 2.73×10^6 ergs/cc ($H_K=11.6$ kOe) and 1.92×10^6 ergs/cc ($H_K=8.2$ kOe), respectively.

For the ⟨100⟩ oriented film, it was shown[4] that applying a similar model of stress (i.e., two in-plane orthogonal stresses along the ⟨100⟩ directions) results in no induced anisotropy in the plane of the film. However, an additional anisotropy is present in out-of-plane measurements, which include the ⟨100⟩ direction normal to the film surface and any direction within the film surface. This anisotropy has $\sin 2\theta$ dependence for the torque and is derived in a manner similar to that described for the ⟨110⟩ oriented film. It has a magnitude $|(3/2)\lambda_{100}\sigma|=3.03\times10^5$ ergs/cc ($H_K=1.3$ kOe) with the easy direction being the ⟨100⟩ direction normal to the film surface. Here σ is the calculated stress along the in-plane ⟨100⟩ direction. The calculated value for the anisotropy constant measured in a plane including the direction normal to the film surface and any direction in the film plane

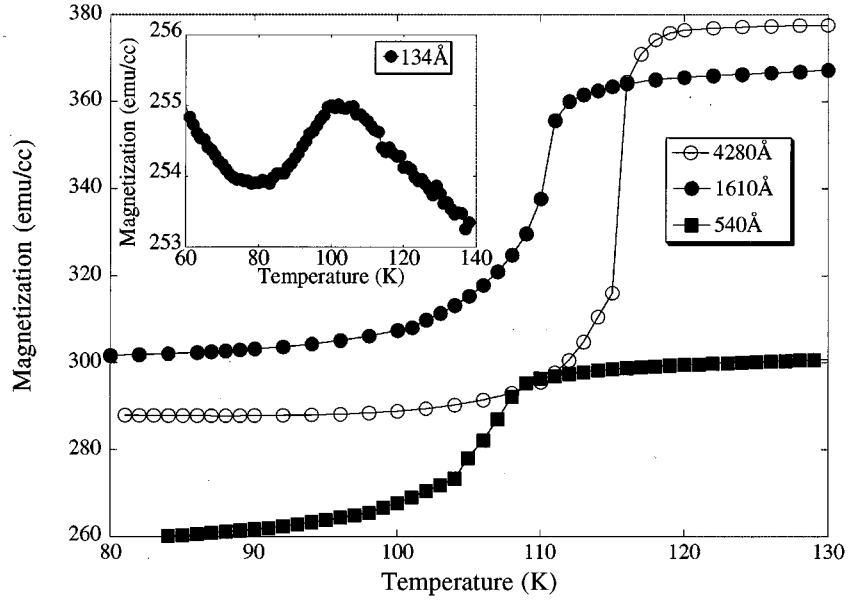

FIG. 10. Magnetization measured along a ⟨100⟩ in-plane direction at a constant field of 1 kOe as the temperature is decreased for the series of Fe_3O_4 films $1a-1d$ (Table I) grown on ⟨100⟩ MgO. The sudden drop in the magnetization is related to the Verwey transition. The lines are visual guides.

is 1.09×10^6 ergs/cc ($H_K=4.6$ kOe) with a small difference between the (110) and the (010) planes from magnetocrystalline anisotropy.[21]

Some measured and extrapolated values, along with the model calculation results, are summarized in Table II. The agreement between the measured and calculated values, in both magnitude and easy direction, is actually quite good considering the many parameters involved in the calculation of the magnetoelastic anisotropy and the assumptions made. This strongly indicates that the differences in the directionally dependent anisotropy between our films and an unstrained single crystal film of bulk Fe_3O_4 are well explained by an added magnetoelastic energy component. It appears that the extrapolated and calculated magnetoelastic anisotropies differ by less than a factor of 2, and the extrapolated shape and crystalline anisotropy are fairly close to bulk values. Another point is that the ⟨100⟩ oriented films (with the added perpendicular strain anisotropy) exhibit a tendency for the moments in zero applied field to lie perpendicular to the film plane (with the CEMS parameter $p\sim0.75$), and the ⟨110⟩ oriented films (with the added in-plane strain anisotropy) exhibit a tendency to have the moments lie in the plane of the film ($p\sim1.6$). However, for both orientations, including the magnetoelastic energy correction, the moments should lie completely in the film plane.

Verwey transition

Stoichiometric Fe_3O_4 undergoes a structural change from cubic to monoclinic[29] below the Verwey transition near 121 K,[30] which is accompanied by a change in the anisotropy.[31] When Fe_3O_4 is cooled through the Verwey transition temperature T_v in a small magnetic field, a sharp decrease in the magnetization is observed.[18] Figure 10 shows magnetization as a function of temperature when the ⟨100⟩ oriented films $1a-1d$ are cooled in a constant field of 1 kOe applied in the ⟨100⟩ direction within the film plane. The transition temperature for all films is lower than 121 K, decreases with film thickness, and is almost unobservable in the 134 Å film. The measured Verwey transition temperatures, as defined by the maximum in $|dM/dT|$, are shown in Table I for many of the films discussed. The decrease in T_v with film thickness was observed in series 1 specimens (both orientations) and series 2 specimens. The ⟨110⟩ oriented films had slightly higher values of T_v than the ⟨100⟩ oriented films grown at the same time (series 1). In Table I one can see that T_v increased when the substrate was positioned closer to the target (lowered further into the plasma), but further attempts at changing the O_2 pressure during deposition and the target-to-substrate distance did not increase T_v. The measured T_v for the bulk single crystal specimen was 101 K.

It has been shown[30] that slight deviations from stoichiometry in bulk samples produce decreases in T_v. For example, for $Fe_{3(1-\delta)}O_4$, $T_v=115$ K when $\delta=1.7\times10^{-3}$, and $T_v=90$ K when $\delta\sim1\times10^{-2}$. The deviation from stoichiometry associated with the reduced T_v is generally associated with Fe^{2+} vacancies on the B site.[25] These vacancies exist in iron oxide as it is oxidized from Fe_3O_4 through the berthollide $Fe_{3(1-\delta)}O_4$ phase to γ-Fe_2O_3. The Fe_3O_4 films exhibit a decreased T_v which might indicate the presence of a small fraction of vacancies. It must be noted that the strain present in the films grown on MgO⟨100⟩ at 296 K is already larger than the strain[29] accompanying the structural change of bulk Fe_3O_4 as the temperature is lowered through T_v. Therefore, it may not be valid to compare T_v of epitaxially constrained films to the T_v of bulk $Fe_{3(1-\delta)}O_4$ and then infer the deviations in stoichiometry.

It is possible that these putative cation vacancies are the origin of all the anomalous magnetic behavior. We note, however, that the bulk sample has a much lower T_v than the film specimens, indicating the presence of a greater fraction of vacancies than the films, yet this specimen is fully saturated in high fields (Fig. 3). Also, Aragon[18] measured the difference in magnetization at 10 kOe with values extrapolated to infinite field, to be less than 1% for bulk specimens with δ as large as 6×10^{-3}. Furthermore, the film grown by MBE, and indicated to be stoichiometric by measurements of T_v (see Table I), exhibits the same anomalous moment distribution as measured by CEMS (Table I), and also shows

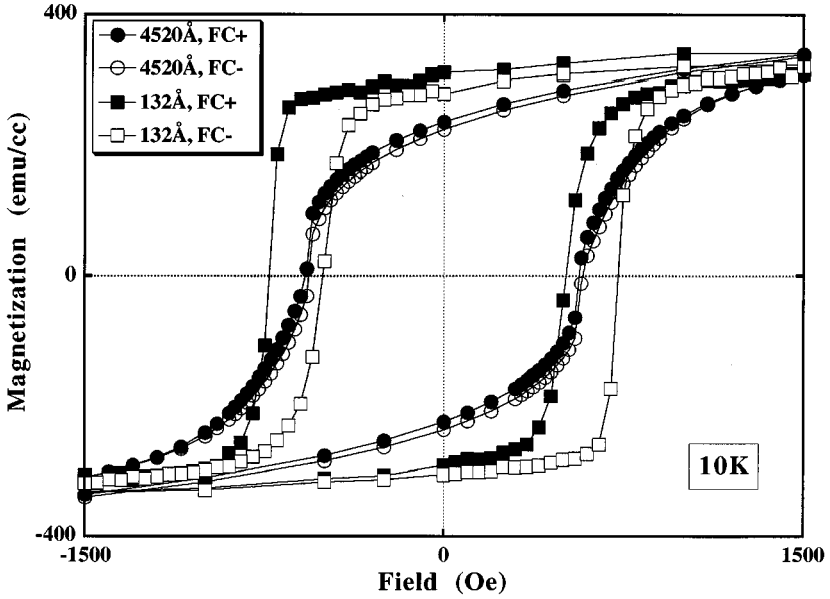

FIG. 11. The magnetization measured along an in-plane ⟨100⟩ direction as a function of field at 10 K for the Fe_3O_4 films 3*a*,3*b* (Table I) grown on ⟨100⟩ MgO after the films have been cooled in a field of ±10 kOe from 300 K. In the figure the *M*-*H* curves after the +10 kOe and −10 kOe field cool are labeled FC+ and FC−, respectively. The curves extend to ±70 kOe (not shown). The lines are visual guides.

similar lack of saturation of the magnetization at high fields as do the sputtered films. Therefore, it does not appear that cation vacancies are the origin of the anomalous behavior. Considering how small the deviation from stoichiometry is in these films, as indicated by T_v, it appears as if the films are actually very close to stoichiometric Fe_3O_4. The surface and the interface may be nonstoichiometric, perhaps ''non-Fe_3O_4'' regions, which could partly be the cause of the decrease of T_v with thickness.

Shifted loops

Figure 11 shows the *M*-*H* curves for the ⟨100⟩ oriented films 3*a*,3*b* after cooling to 10 K in a ±10 kOe magnetic field from 300 K. When a film is cooled in a positive field the *M*-*H* curve is shifted in the negative field direction; when a film is cooled in a negative field the *M*-*H* curve is shifted in the positive field direction. For film 3*b* this shift is 110 Oe and the coercivity is 620 Oe, while for film 3*a* the shift is 7 Oe, and the coercivity is 575 Oe. Although the shift, relative to the coercivity, is small for film 3*a* it is clearly observable when the ±10 kOe field-cooled *M*-*H* curves are compared. Other nominally 0.4 μm films, which exhibit lower measured values for K_1 and larger W_r, have larger shifts at 10 K. The shift disappears at ~200 K. Similar behavior is also observed at 10 K in the 6.6 μm film. Field cooling experiments with the bulk Fe_3O_4 sample resulted in no visible shift in the loop, but the remanence ratio was only 1% and coercivity was 27(1) Oe.

Materials which exhibit shifts in their magnetization loops at low temperatures when cooled in the presence of a magnetic field are usually associated with a system containing two magnetic phases.[32] Therefore, it is interesting that the ordering temperature of FeO is 198 K. However, XRD, CEMS, and TEM show the presence of only single phase Fe_3O_4 so an FeO phase does not appear to be the origin of the shift. Although the shift in the field-cooled *M*-*H* curve decreases with increasing thickness, it does not disappear in the 6 μm films, so the shifted loop is not strictly a surface or interface effect. Although the bulk specimen displayed no shift in the field-cooled *M*-*H* curve, the specimen had a much lower coercivity than the films, so the shift may not be measurable. Rotational hysteresis, which is related to the shifted loop mechanism,[32] has been reported[33] for natural single crystals of Fe_3O_4 samples below T_v. Therefore, it is not clear if the shift is found only in film specimens and consequently may not be related to the anomalous behavior.

Other studies

This section discusses the results of growing films under other conditions and the influence of subsequent heat treatments, concentrating on ⟨100⟩ oriented films with thicknesses of ~0.3 μm. The magnetization values of single phase Fe_3O_4 films grown at 650 and 100 °C were unsaturated, and were lower at 70 kOe than the films described above. Films within this temperature deposition range all exhibit unsaturated magnetization at 70 kOe and quasirandom moment distribution in the CEMS spectra. This indicates the anomalous behavior is independent of substrate temperature. A series of films were also grown at 500 °C with an 18 cm target-to-substrate distance under conditions in which the O_2 pressure was varied during deposition from 0.03 mtorr (resulting in a mixture of Fe and Fe_3O_4), to a pressure of 0.18 mtorr (resulting in α-Fe_2O_3/Fe_3O_4 phase mixtures). Although these films indicated a dependence on the measured values of K_1 with $P(O_2)$, the properties of films in the Fe_3O_4 single phase region in this series were qualitatively all the same, i.e., the magnetization was unsaturated and the CEMS spectra exhibited near random moment distribution. This indicates the anomalous behavior is present in the films independent of the O_2 pressure during deposition.

Post deposition heat treatments were also studied. One Fe_3O_4 film was annealed in a moderately reducing, flowing H_2/H_2O atmosphere at 350 °C for 1 h. No changes in the approach to saturation, CEMS spectrum, or T_v were detected. Further reduction at 550 °C, under the same conditions, resulted in Fe metal. Another film was annealed at 600 °C in a vacuum of 2×10^{-10} torr with no change in the approach to saturation or T_v. After annealing at 800 °C in

the same vacuum, the magnetization remained unsaturated and a further 20% reduction in the magnetization was observed. CEMS spectra, sensitive to about the upper third of the film, showed the presence of only the Fe_3O_4 phase, and a θ-2θ XRD scan showed a 50% increase in the FWHM of the symmetric 800 reflection. These results could arise from diffusion of Mg from the substrate into the film. Annealing in an O_2/H_2O atmosphere at 120 °C for 2 h resulted in no change in the magnetic properties. Annealing under the same conditions at 220 °C decreased T_v and the magnetization remained unsaturated. In fact, preliminary results indicate the anomalous behavior to be still present in films oxidized completely to the γ-Fe_2O_3 phase. Annealing a 500 Å film at 500 °C and 2.00 mtorr of Ar for 5 h produced the quasirandom CEMS polarization and only the Fe_3O_4 phase. It is unlikely that any substantial diffusion occurred at the interface since no other phases containing Fe were observed. Furthermore, the ⟨100⟩ oriented 134 Å film 1d was measured with Auger spectroscopy and no Mg was observed at the film surface with an upper limit of the Mg/Fe ratio estimated to be ~1%.

DISCUSSION

The magnetic properties of Fe_3O_4 films are obviously anomalous. The magnetizations do not saturate in applied magnetic fields as high as 70 kOe and the torque curves do not saturate in applied magnetic fields of 21 kOe. Moreover, the CEMS spectra show that the moments are not lying in the film plane in zero applied field as expected from the shape anisotropy field. However, the extrapolated values for all the anisotropies with measurable directional dependence for the films grown on MgO are much less than the magnitude of an anisotropy which would be needed to cause these effects. Moreover, the directionally dependent anisotropies agree in symmetry, and reasonably well in magnitude, with the experimentally based model of a single crystal Fe_3O_4 subjected to in-plane tensile stress, and shape anisotropy is the dominant anisotropy. Furthermore, all of the Mössbauer parameters measured, such as the hyperfine fields, the isomer shifts, and site occupancies, are consistent with the films being single phase bulk Fe_3O_4, and yet the anomalous behavior of the films appears to be incommensurate with the parameters of bulk Fe_3O_4.

At this point it appears that several possible structural origins of the anomalous behavior are not present. First of all, we have yet to observe defects in the films grown on MgO. Defects randomly distributed throughout the film could conceivably be associated with a large anisotropy randomly distributed throughout the film. A locally large, but globally random anisotropy, could lead to a canting of the moments and would be consistent with many of the magnetic properties measured. A second possible structural origin is the presence of antiphase boundaries which could result during the epitaxial growth of Fe_3O_4 on MgO. Fe_3O_4 has twice the unit cell size of MgO, even though it crystallizes with approximately the same fcc oxygen lattice as MgO. Therefore, if the Fe_3O_4 were growing by island nucleation, when the islands grow together the correct stacking sequence of the spinel structure could occur with the same probability as the stacking sequence being half a unit cell out of phase. A shift in the stacking sequence, i.e., antiphase boundaries, would interfere with the normal exchange in Fe_3O_4 and could lead to a canted spin structure which would be consistent with the large saturation fields. Although these structural defects have yet to be observed, we do not dismiss the possibility of their presence. We suspect that the anomalous behavior indeed has structural origins and we are continuing our structural characterization of the films.

Another origin for a large anisotropy which could lead to anomalously large saturation fields is magnetoelastic energy from the strain in the film. However, our strain model for the films grown on MgO seems to account very well for the magnetoelastic anisotropy in these films, and the magnitudes of the measured and calculated magnetoelastic anisotropies are much smaller than those which would be needed to cause the high saturation fields. Furthermore, no directional dependence is observed for the high field behavior, yet a directional dependence is expected in the single crystal films. A nonuniform strain could conceivably result in a large anisotropy randomly distributed throughout the crystal or frustration in the exchange, leading to these behaviors, but from the FWHM of the rocking curves the strain appears to be exceptionally uniform. Therefore, magnetoelastic anisotropy does not appear to be the origin of the anomalous behavior.

The anomalous properties are present in all films measured and appear to be an intrinsic property of all Fe_3O_4 films. They are present independent of substrate and of deposition conditions, as well as of some post deposition treatments. There does appear to be a thickness dependence in many of the properties, especially the measured anisotropy, but the qualitative results appear not to show a thickness dependence. Therefore, the anomalous behavior appears to be principally a volume effect with a much smaller superimposed surface-related anomaly. Also, the properties of the films grown by MBE and evaporation are similar to those of these sputtered films.

Apparently, the origin of the anomalous behavior is the same for the films grown on all substrates; it is the same for polycrystalline and single crystal films. Since defects have not yet been observed in the single crystal films, a similarity between the polycrystalline and single crystal films is that they are all under a considerable amount of strain and have not relaxed to the bulk value even in the thickest films. This may indicate that the strain is related to the anomalous behavior.

Two possibilities may be considered with respect to the strain. First of all, the XRD measurements we have performed are dominated by the iron lattice in the film. Therefore, we do not know how the oxygen lattice is responding to the strain. We are investigating the possibility of a distortion in the oxygen lattice that may be the origin of the behavior in the films. Although, qualitatively, the properties of the films at grown at different oxygen pressures $P(O_2)$ all exhibit the anomalous behavior, we do measure a dependence of the measured value of K_1 on $P(O_2)$ which could indicate the presence of a feature in the oxygen lattice we have not observed. Secondly, it not clear what effect the strain has on the exchange in the film. It is conceivable that the tetragonal distortion, or a further distortion in the oxygen lattice, has

produced a noncollinear spin structure.[34] The magnitude of the effect, i.e., the fact that the film will not saturate in fields larger than 70 kOe, seems to point toward exchange as the origin.

One point which should be useful in modeling the properties of these films comes from the CEMS data. The distortions in the films grown on the two orientations of MgO, although both are tetragonal, lead to much different symmetries in the films. For instance, in a ⟨110⟩ oriented film the crystallographic axes of the film unit cell are no longer parallel to the crystallographic axes of the unstrained bulk unit cell, while in a ⟨100⟩ oriented film they are. In the CEMS data the polarization values, which are determined by the angles of the moments to the planes of the films, are much different for the two orientations. The CEMS data are consistent with the moments lying along specific crystallographic directions. For a ⟨100⟩ oriented film there is a ⟨110⟩ direction with an angle of 45° to the surface and for a ⟨110⟩ oriented film there is a ⟨110⟩ direction with an angle of 60° to the surface. Both of these angles are close to the effective angles measured by CEMS for the respective films. However, considering the magnitudes of the directionally-dependent anisotropies measured, we see no reason why the moments should be lying in these specific directions. Therefore, at least several directions are most probably involved. However, the large difference in polarization between the two orientations, and the similarity in the polarization for the films grown on ⟨100⟩ MgO by different deposition techniques, may indicate that a specific spin structure or domain structure is being attained in these films and that the moment distribution is not a variation on a random distribution.

CONCLUSION

Fe_3O_4 films grown on MgO substrates by sputter deposition are epitaxial single crystal specimens. CEMS spectra exhibit bulk values for the hyperfine fields, isomer shifts, and relative occupancy of the *A* and *B* sites. However, magnetization and torque curves remain unsaturated in large fields, and CEMS spectra show an anomalous out-of-plane moment distribution. Still, extrapolated values of all of the directionally dependent anisotropies are consistent with the magnetocrystalline, magnetoelastic, and shape anisotropies of Fe_3O_4 single crystals subjected to in-plane tensile stress, and the magnitudes of these values are much less than that needed to result in the unsaturated high field measurements. A structural defect which could produce this behavior has yet to be observed and this behavior does not appear to be related to magnetoelastic anisotropy. The anomalous behavior is present independent of thickness, substrate, further heat treatments, deposition conditions, and deposition technique, and appears to be an intrinsic property of all Fe_3O_4 films.

ACKNOWLEDGMENTS

The authors would like to thank David Lind for providing the MBE grown sample, Mark Rubenstein for providing the bulk Fe_3O_4 specimen, and Sihong Kim for help with the annealing experiments measurements, William Margulies for assistance with tensor calculations, Stefano Spagna for assistance with Auger measurements, and Pekir Aktas for first demonstrating the existence of the shift in the *M*-*H* curve at low temperatures. This work was supported by NSF Grant No. DMR 9400439 and by the National Media Laboratory. R.S.G. acknowledges financial support of the Office of Naval Research.

*Present address: Department of Physics, Carnegie-Mellon University, Pittsburgh, PA 15213.

[1] D. M. Lind, S. D. Berry, G. Chern, H. Mathias, and L. R. Testardi, Phys. Rev. B **45**, 1838 (1992).

[2] E. Lochner, K. A. Shaw, R. C. Dibari, W. Portwine, P. Stoyonov, S. D. Berry, and D. M. Lind, IEEE Trans. Magn. **30**, 4912 (1994).

[3] D. M. Lind, S. D. Berry, G. Chern, H. Mathias, and L. R. Testardi, J. Appl. Phys. **70**, 6218 (1991).

[4] D. T. Margulies, F. T. Parker, and A. E. Berkowitz, J. Appl. Phys. **75**, 6097 (1994).

[5] D. T. Margulies, F. T. Parker, F. E. Spada, and A. E. Berkowitz, in *Epitaxial Oxide Thin Film and Heterostructures*, edited by D. K. Fork *et al.*, MRS Symposia Proceedings No. 341 (Materials Research Society, Pittsburgh, 1994), p. 53.

[6] T. Fujii, M. Takano, R. Katano, and Y. Bando, J. Cryst. Growth **99**, 606 (1990).

[7] T. Shigematsu, H. Ushigome, Y. Bando, and T. Takada, J. Cryst. Growth **50**, 801 (1980).

[8] V. S. Speriosu, M. M. Chen, and T. Suzuki, IEEE Trans. Magn. **25**, 3875 (1989).

[9] C. A. Kleint, H. C. Semmelhack, M. Lorenz, and M. K. Krause, J. Magn. Magn. Mater. **140–144**, 725 (1995).

[10] Y. K. Kim and M. Olivera, J. Appl. Phys. **75**, 431 (1993).

[11] R. M. Wolf, A. E. M. De Veirman, P. van der Sluis, P. J. van der Zaag, and J. B. F. aan de Stegge, in *Epitaxial Oxide Thin Films and Heterostructures*, edited by D. K. Fork *et al.*, MRS Symposia Proceedings No. 341 (Materials Research Society, Pittsburgh, 1994), p. 23.

[12] B. D. Cullity, *Introduction to Magnetic Materials* (Addison-Wesley, Reading, MA, 1972), p. 233.

[13] *Thin Films from Free Atoms and Particles*, edited by K. J. Klabunde (Academic, Orlando, FL, 1985), p. 344.

[14] J. C. Bravman and R. Sinclair, J. Electron Microsc. Tech. **1**, 53 (1984).

[15] *Powder Diffraction File: Inorganic Phases*, edited by W. F. McClune (International Centre for Diffraction Data, Swarthmore, PA, 1989).

[16] S. Chikazumi, *Physics of Magnetism* (Robert E. Krieger Publishing Company, Malabar, FL, 1986), pp. 274–280.

[17] *Magnetic and Other Properties of Oxides and Related Compounds*, edited by K.-H. Hellwege and A. M. Hellwege, Landolt-Börnstein, New Series, Vol. 4 (Springer-Verlag, Berlin, 1970).

[18] R. Aragon, Phys. Rev. B **46**, 5328 (1992).

[19] H. B. Callen and E. Callen, J. Phys. Chem. Solids **27**, 1271 (1966).

[20] B. J. Evans and S. S. Hafner, J. Appl. Phys. **40**, 1411 (1969).

[21] B. D. Cullity, *Introduction to Magnetic Materials* (Addison-Wesley, Reading, MA, 1972), pp. 215–224.

[22] *Magnetism and Metallurgy*, edited by A. E. Berkowitz and E. Kneller (Academic, New York, 1969), pp. 418–427.

[23] J. Castro, J. Rivas, and H. J. Blythe, J. Magn. Magn. Mater. **131**, 311 (1994).
[24] J. Castro, J. Rivas, H. J. Blythe, J. Iniguez, and C. De Francisco, Phys. Status Solidi A **113**, 541 (1989).
[25] H. Kronmüller, R. Schutzenauer, and F. Waltz, Phys. Status Solidi A **24**, 487 (1974).
[26] A. Broese van Groenou, J. L. Page, and R. F. Pearson, J. Phys. Chem. Solids **28**, 1017 (1967).
[27] S. Chikazumi, *Physics of Magnetism* (Robert E. Krieger Publishing Company, Malabar, FL, 1986), p. 183.
[28] J. F. Nye, *Physical Properties of Crystals* (Clarendon, London, 1964).
[29] J. Yoshida and S. Iida, J. Phys. Soc. Jpn. **47**, 1627 (1979).
[30] J. P. Shepherd, J. W. Koenitzer, R. Aragon, J. Spalek, and J. M. Honig, Phys. Rev. B **43**, 8461 (1991).
[31] S. Chikazumi, *Physics of Magnetism* (Robert E. Krieger Publishing Company, Malabar, FL, 1986), pp. 387–389.
[32] W. H. Meiklejohn, J. Appl. Phys. **33s**, 1328 (1962).
[33] R. F. Pearson and R. Cooper, Proc. Phys. Soc. **78**, 17 (1960).
[34] J. M. D. Coey, Can. J. Phys. **65**, 1210 (1987).